N94-17338

Diffractive Optical Elements for Generating Arbitrary Line Foci

Joseph N. Mait, Dennis W. Prather, Joseph van der Gracht, and Tristan J. Tayag
U.S. Army Research Laboratory
AMSRL-SS-SF
2800 Powder Mill Road
Adelphi, Maryland 20783

1. Introduction

The key optical component in the architecture of the linearly variable magnification telescope shown in Fig. 1 is a conical lens. This architecture has application to Doppler radar processing and to wavelet processing. Unfortunately, the unique surface profile of a conical lens does not allow traditional grinding techniques to be used for fabrication and therefore its fabrication is considered custom. In addition to the requirement of custom fabrication, a refractive conical lens introduces phase aberrations that are intrinsic to its conic shape. Further, due to the large prismatic component of the lens, the variable magnification telescope architecture is off-axis.

To overcome the fabrication and application difficulties of a refractive lens, we consider the construction of a hybrid diffractive-refractive lens that has a phase profile given by

$$\phi(u,v) = \frac{2\pi}{\lambda}\,[f(v) - \sqrt{f^2(v)+u^2}], \tag{1}$$

where the focal length $f(v)$ is an arbitrary function of v and λ is the wavelength of illumination. The effect of such an arbitrary line foci element (ALFE) is to produce a focal line in three-dimensions whose shape along the axis of propagation follows that of the function $f(v)$. Cylindrical and conical lenses are the most common refractive elements that are capable of producing focal lines.

To generate the focal line $f(v)$ we consider a hybrid element that consists of a refractive element that generates the focal line $f_R(v)$ and a diffractive lens that generates the focal line $f_D(v)$:

$$\frac{1}{f_R(v)} + \frac{1}{f_D(v)} = \frac{1}{f(v)}. \tag{2}$$

If the refractive element is used to provide a constant optical power, $f_R(v) = f_R$, i.e., the refractive element is a cylindrical lens, constraints on the fabrication of the diffractive lens can be reduced. For example, an ALFE that varies in focal length from 160 mm to 240 mm over a 50×50 mm^2 aperture varies in f-number from 3.2 to 4.8. If $f_R = 325$ mm, the cylindrical lens is $f/6.5$ and the diffractive lens varies in f-number from 6.3 [$f(0) = 315$ mm] to 18.35 [$f(50) = 917.5$ mm], which is less difficult to fabricate than lower f-number lenses.

We now consider the design of a thin phase-only diffractive optical element (DOE) $P(u,v)$,

$$P(u,v) = \exp[j\phi_D(u,v)], \tag{3a}$$

that is capable of generating the focal line $f_D(v)$. A multi-level quantized phase-only DOE is assumed,

$$\phi_D(u,v) = \sum_{n=0}^{N}\sum_{m=0}^{M} \phi_{nm,L}\ \mathrm{rect}(\frac{u-u_n}{\Delta}, \frac{v-v_m}{\Delta}), \tag{3b}$$

where Δ is the minimum feature size of the pattern generator used to produce the binary masks and

$$\phi_{nm,L} \in [0, \frac{2\pi}{2^L}, 2\frac{2\pi}{2^L}, \ldots, (2^L-1)\frac{2\pi}{2^L}]. \tag{3c}$$

The resolution with which each phase pixel can be positioned is defined by the placement accuracy ϵ of the pattern generator, i.e., $u_n = \ell\epsilon$ and $v_n = k\epsilon$. The ability of $P(u,v)$ to generate a high-fidelity focal line $f_D(v)$ is limited by the minimum feature size Δ of the pattern generator, its placement accuracy ϵ, and the number of phase quantization levels 2^L. Design of the diffractive ALFE entails the determination of the parameters $\phi_{nm,L}$ and (u_n, v_n), from which L binary masks are produced.

We consider the design of a diffractive ALFE based on the sampling and quantization of $\phi_D(u,v)$ and experimental results from a binary-phase ALFE designed in this manner are presented. We also consider two alternative design approaches: a second approach based on sampling and quantization and an iterative approach that detemines the parameters by optimizing some design metric. The difficulties encountered in lens design and characterization of lens performance are addressed.

2. Deterministic Design

In the literature, the design of diffractive lenses implies the design of spherical lenses, which, by exploiting spherical symmetry, can be reduced from a two-dimensional problem to one that is one-dimensional. For diffractive ALFE design, symmetry properties can not be exploited to reduce the dimensionality of the design problem. Rather, dimensionality reduction is realized by noting that the phase function at every u-axis slice of the diffractive ALFE is a spatially scaled version of a one-dimensional lens:

$$\phi_D(u,v) = s(v)\ \phi_D[\frac{u}{s(v)}, 0], \tag{4a}$$

where $s(v)$ represents a normalized focal function,

$$s(v) = \frac{f_D(v)}{f_D(0)}. \tag{4b}$$

The even nature of the ALFE, i.e., $\phi_D(u,v) = \phi_D(-u,v)$, can be used to halve the number of design parameters.

Lens design is realized by quantizing lines of constant phase:

$$u_i(v) = \sqrt{\frac{\lambda\phi_i}{2\pi}\left[\frac{\lambda\phi_i}{2\pi} - 2f_D(v)\right]}, \tag{5a}$$

where

$$\phi_i = \frac{2\pi i}{2^L},\ i = [1, I]. \tag{5b}$$

The number of phase lines I to be quantized is dependent upon the minimum phase value obtained by $\phi_D(u,v)$:

$$I = \text{ROUND}\left[\frac{2^L}{2\pi}\min\{\phi_D(u,v)\}\right], \tag{5c}$$

where ROUND implies rounded to the nearest integer. The minimum phase is, in turn, related to the minimum f-number one-dimensional lens described by $\phi_D(u,v)$. If the DOE aperture is allowed to vary with $f(v)$ then the diffractive ALFE maintains a constant f-number and each lens has the same number of phase lines. However, to allow the aperture to vary represents an inefficient use of the overall aperture. On the other hand, a constant aperture generates variable f-number one-dimensional lenses and produces a focal line that has variable spot size and brightness. The tradeoff between aperture efficiency and focal line fidelity needs to be consider for each application. We assume that the aperture is constant and is defined by the aperture of the refractive cylindrical lens.

One method for implementing the design, referred to as the direct sampling (DS) method, is to ignore the effect of ϵ and quantize the lines $u_i(v)$ according to the minimum feature size Δ. For the DS method, L and Δ_x dictate the minimum f-number of the lens that can be designed and L dictates the lens diffraction efficiency [1,2]. In effect, the DS method assumes that $\phi_D(u,v)$ is sampled on a regular Cartesian grid and is then quantized. The spacing of the grid is determined by the minimum feature size of the pattern generator used to produce the binary masks.

Figure 2(a) is the DS-generated binary mask for a conical lens that has a linear change in focal length from 300 mm to 480 mm over a 4 × 4 mm² aperture. The focal length increases in 3.6 mm increments over the aperture, thus, the ALFE consists of 50 one-dimensional lenses. The minimum feature size is 10 μm. The lens was fabricated on a Corning glass substrate that has an index of refraction $n = 1.53$ using a 1.8 μm layer of positive photoresist (Hoechst AZ 5214) and an Ar ion etch. The axial performance of the lens is represented in Figs. 2(b)-(d), which indicates that the focal length actually changes from approximately 220 mm to 350 mm.

Due to the varying axial behavior of the lens, it is difficult to characterize its performance. For a spherical lens, in most instances, it suffices to take a measure of the diffraction efficiency, the percentage of input light energy that is brought to focus. For an ALFE, the diffraction efficiency must be measured along the focal line:

$$\eta(y) = \int_{\mathbf{X}} |U[x, y; f(y)]|^2 \, dx \Big/ \int |U[x, y; f(y)]|^2 \, dx \tag{6}$$

where $\mathbf{X}$ is the width of the focal spot and $U(x, y; z)$ is the complex wave-amplitude field generated by $P(u,v)$ at an arbitrary distance z in the near-field,

$$U(x, y; z) = \frac{1}{j\lambda} \exp\left(j\frac{2\pi z}{\lambda}\right) \int\int_{\mathbf{A}} \exp\left[j\phi_D(u,v)\right] \exp\left\{j\frac{\pi}{\lambda z}[(u-x)^2 + (v-y)^2]\right\} du\, dv. \tag{7}$$

The area of the ALFE aperture is denoted by $\mathbf{A}$. To reduce the computational load in evaluating the three-dimensional function $U(x, y; z)$, if y-axis diffraction is ignored, Eq. (7) can be simplified

$$U[x, y; f(y)] = \frac{1}{j\lambda} \exp\left[j\frac{2\pi f(y)}{\lambda}\right] \int_{W_u} \exp\left[j\phi_D(u,y)\right] \exp\left[j\frac{\pi}{\lambda f(y)}(u-x)^2\right] du, \tag{8}$$

where W_u is the u-axis aperture of the ALFE. The diffraction efficiency along the focal line generated by the DS conical lens as determined using Eq. (8) is presented in Fig. 3.

Diffraction efficiency can be increased if the placement accuracy ϵ is not ignored. In other words, although the minimum feature size is fixed, the accuracy with which the lines of constant phase are quantized can be sampled on a finer grid determined by the placement accuracy. Fabrication of the masks, though, is still limited by the minimum feature size of the pattern generator. As represented in Fig. 4, to realize this finer quantization multiple exposures are used to generate the masks necessary for fabrication, but, because the masks are binary, multiple exposures do not affect mask transmission. This design technique is referred to as analytic quantization (AQ).

The distinction between DS- and AQ-designed ALFEs is evident in Fig. 5 and the increase in diffraction efficiency is represented in Fig. 6. The ALFE is characterized by a focal length change from 256 μm to 1040 μm in 19.6 μm increments (40 lenses) over a 80 × 80 μm² aperture. Minimum feature size is assumed to be 2 μm with a placement accuracy of 0.2 μm. The percent change in diffraction efficiency ranges from a minimum of zero to a high of 35% and is most notable for low f-number lenses, which have higher phase curvature than high f-number lenses. Note that the improvement in diffraction efficiency is reduced for those lenses that experience "edge effects" introduced by the minimum feature size limitation. Unfortunately, consideration of the placement accuracy during design increases by 100 the amount of data necessary for fabrication of a single mask. Thus, whereas the lens in Fig. 5(a) contains only 40 × 40 data points, the lens in Fig. 5(b) contains 400 × 400.

3. Iterative Design

Although performance characterization of an ALFE requires, in general, the evaluation of Eq. (7), the application to a variable magnification telescope allows us to characterize lens performance based on telescope performance. For telescopic operation, the input and output are collimated, i.e., the input object is located at $-\infty$ and the output image is at $+\infty$, and the lenses are separated by a distance $d = f(0) + f(W_v)$, where W_v is the v-aperture of the lens. Thus, the image $i(x_i, y_i)$ of an input object $o(x_o, y_o)$ produced by the ALFE phase $\phi_D(u,v)$ is

$$\begin{aligned} i(x_i, y_i) &= \frac{-1}{\lambda^2 z} \exp\left[j\frac{2\pi(d+z)}{\lambda}\right] \exp\left[j\frac{\pi}{\lambda z}(x^2+y^2)\right] \int\!\!\int \exp\left[j\phi_D(-u,-v)\right] \qquad (9) \\ &\times \left[\int\!\!\int_{\mathbf{A}} o(x_o, y_o) \exp\left[j\phi_D(x_o, y_o)\right] \exp\left\{j\frac{\pi}{\lambda d}[(x_o-u)^2+(y_o-v)^2]\right\} dx_o\, dy_o\right] \\ &\times \exp\left[\frac{2\pi}{\lambda z}(ux_i + vy_i)\right] du\, dv, \end{aligned}$$

where Fourier transformation is used to represent Fraunhofer diffraction to a distance z in the far-field. For a unit amplitude plane wave input, Fig. 7 represents simulated image reconstructions generated by Eq. (9) for a continuous phase zone plate lens and lenses designed using DS with phase quantization levels of 2, 4, and 8. No cylindrical lens was used and the diffractive lens has a focal change from 240 mm to 384 mm over a 3.2 mm aperture ($f/75$ to $f/120$). The smallest feature is 25 μm. Use of a cylindrical lens only changes the magnification and not the diffractive lens behavior. The magnification changes from 1.6 to 0.625 over the extent of the aperture.

It is apparent from Fig. 7 that a binary-phase DS conical lens is incapable of performing in the telescopic system. Diffractive artifacts are apparent even in the zone-plate image and it is interesting to note that more of the image is filled in as the number of phase quantization levels increases. The effect of variable magnification is also evident by the varying levels of image intensity; as the magnification increases, the intensity level decreases.

To account for the undesirable effects of deterministically designed lenses, it is possible to design $P(u,v)$ using iterative techniques to create a desired output image for a given input object. Because, from Eq. (9), the desired image $q(x_i, y_i)$ can be determined for a given input $o(x_o, y_o)$, it is possible to use iterative techniques, such as simulated annealing [2] and iterative Fourier transform algorithms [3], to determine $\phi_D(u,v)$ such that the error between $i(x_i, y_i)$ and $q(x_i, y_i)$ is a minimum. We will be investigating this technique in the future.

4. Conclusion

We have considered the design of a hybrid diffractive-refractive element that is capable of generating a focal line in space that has an arbitrarily specified shape. The element consists of a refractive cylindrical lens to provide optical power and a diffractive element for shaping the focal line. Although standard design and fabrication techniques have been applied to generate a diffractive conical lens, issues such as performance characterization and design for "improved" performance remain to be addressed more critically. Of utmost importance is data management to reduce design complexity, especially when placement accuracy is used as part of the design. These issues will be addressed in the future.

References

1. G. J. Swanson, *MIT Lincoln Laboratory Technical Report 854*, 14 August 1989.

2. W. H. Welch, J. E. Morris, and M. R. Feldman, "Iterative discrete on-axis encoding of radially symmetric computer generated holograms," submitted to Appl. Opt.

3. F. Wyrowski and O. Bryngdahl, Rep. Prog. Phys., 1481-1571 (1991).

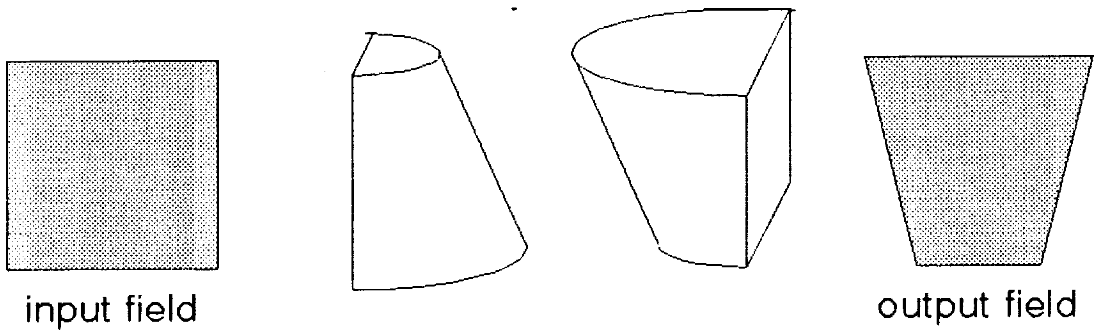

Figure 1. Linearly variable magnification telescope.

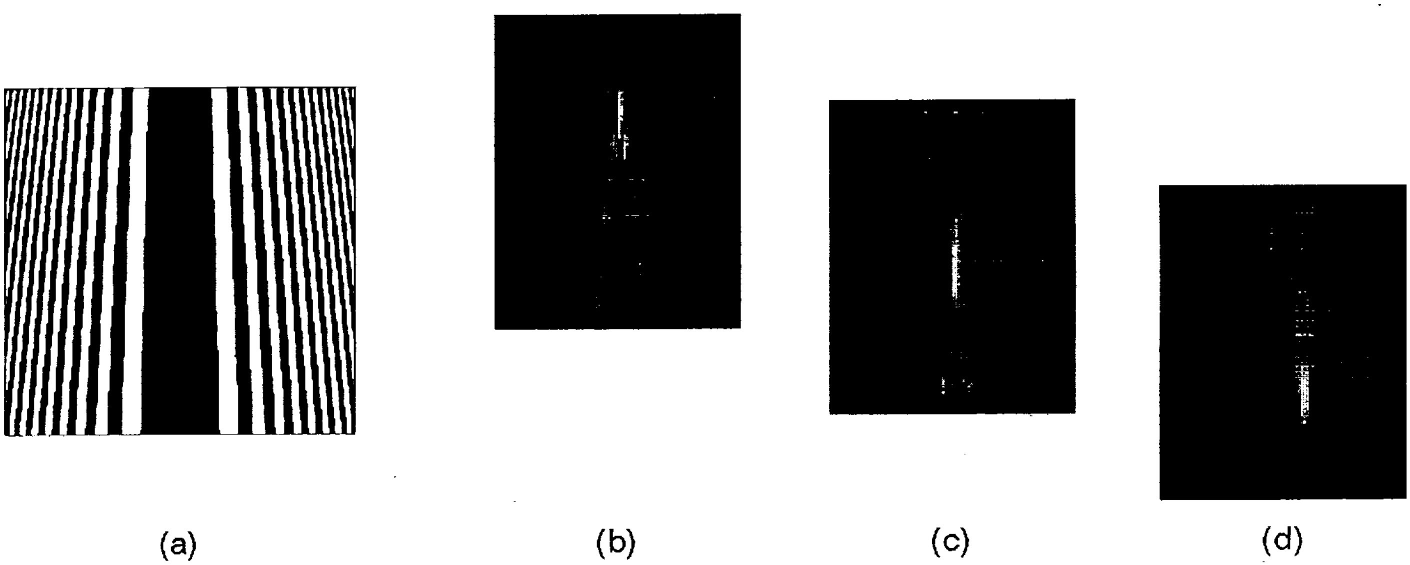

Figure 2. (a) Binary mask designed using DS method and used to fabricate binary-phase conical lens. Lens reconstructions at (b) ~220 mm, (c) intermediate distance, and (d) ~350 mm.

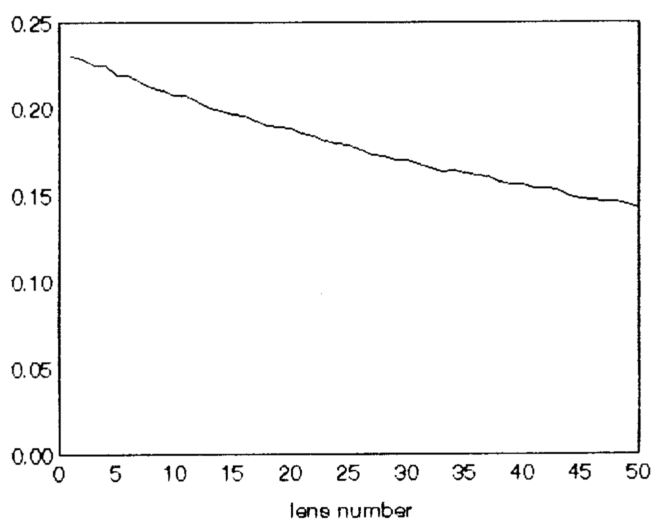

Figure 3. Calculated diffraction efficiency of DS designed binary-phase conical lens.

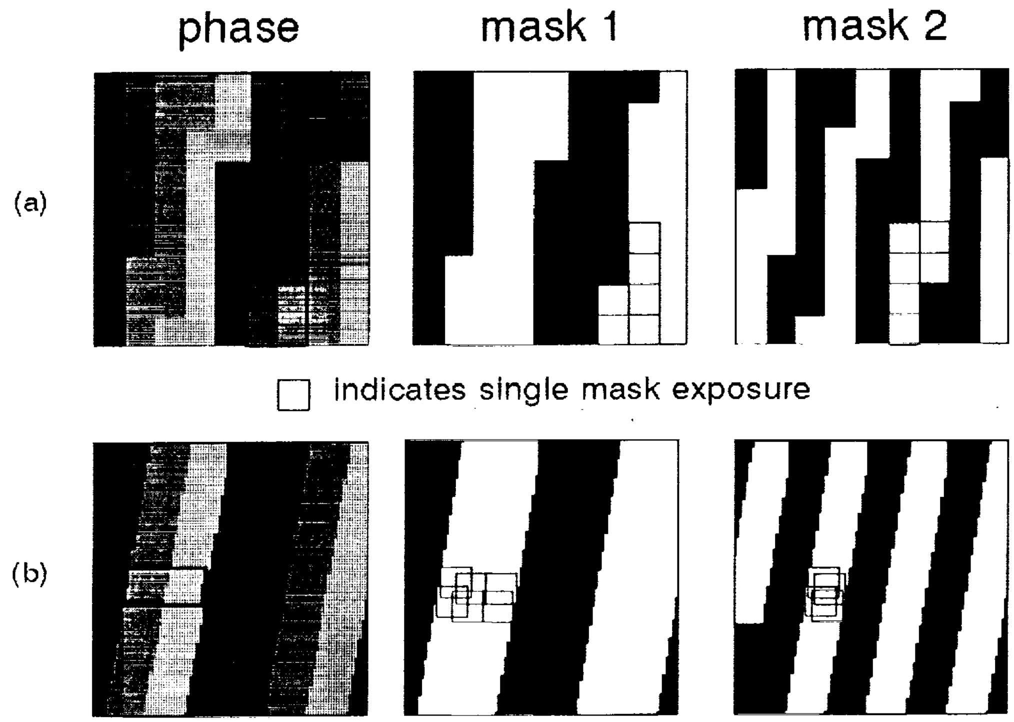

Figure 4. Distinction between (a) direct sampling and (b) analytic quantization design methods.

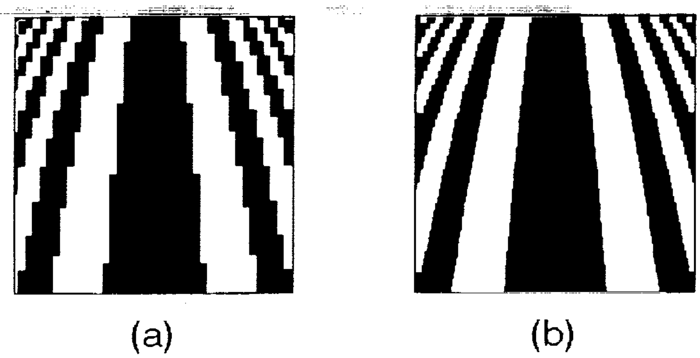

Figure 5. Conical lenses designed using (a) direct sampling and (b) analytic quantization.

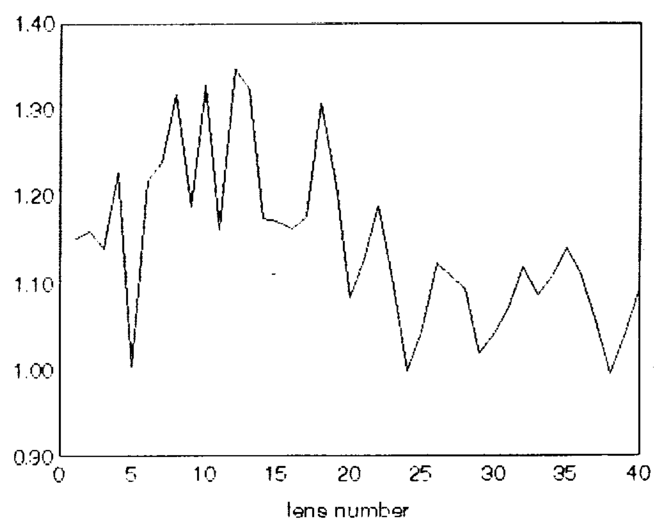

Figure 6. Gain in diffraction efficiency for AQ-designed lens of Fig. 5(b) over DS-designed lens of Fig. 5(a).

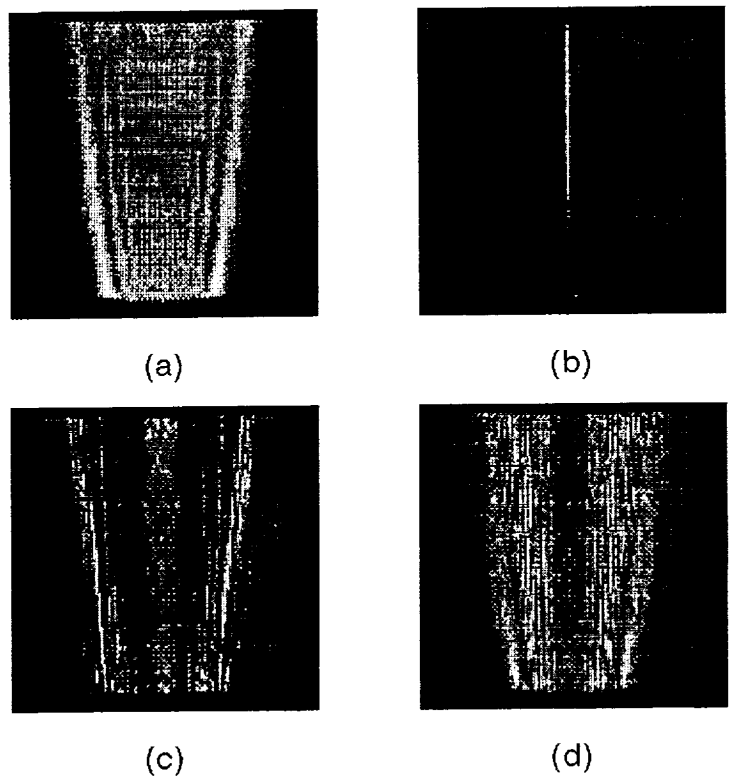

Figure 7. Simulated output image of phase-only conical lens illuminated by unit amplitude plane wave assuming: (a) continuous phase, (b) 2 phase levels, (c) 4 phase levels, and (d) 8 phase levels.